

# The Wolfenstein potential for ultra-light mediators

Alexei Yu. Smirnov<sup>a,b</sup> and Xun-Jie Xu<sup>a</sup>

<sup>a</sup> *Max-Planck-Institut für Kernphysik, Postfach 103980, D-69029 Heidelberg, Germany.*

<sup>b</sup> *International Centre for Theoretical Physics, I-34100 Trieste, Italy.*

(Dated: November 13, 2021)

New physics can emerge at low energy scales, involving very light and very weakly interacting new particles. These particles can mediate interactions between neutrinos and usual matter and contribute to the Wolfenstein potential in neutrino oscillations. We compute the Wolfenstein potential in the presence of ultra-light scalar and vector mediators and study the dependence of the potential on the mediator mass  $m_A$ , taking the finite size of matter distribution (Earth, Sun, supernovae) into consideration. For ultra-light mediators with  $m_A^{-1}$  comparable to the size of the medium ( $R$ ), the conventional  $m_A^{-2}$  dependence of the potential is modified. In particular, when  $m_A^{-1} \gg R$ , the potential does not depend on  $m_A$ . Taking into account existing bounds on light mediators, we find that for the scalar case significant effects on neutrino propagation are not possible, while for the vector case large matter effects are allowed for  $m_A \in [2 \times 10^{-17}, 4 \times 10^{-14}]$  eV and the gauge coupling  $g \sim 10^{-25}$ .

## I. INTRODUCTION

Coherent forward scattering of neutrinos on particles of medium  $\psi$  ( $\psi = e^-, n, p$ ) generates the Wolfenstein potential  $V_W$  [1]. Being added to the neutrino evolution equation,  $V_W$  can significantly affect neutrino oscillations, known as the Mikheyev-Smirnov-Wolfenstein (MSW) effect [1–3]. When neutrino-matter interactions are mediated by a heavy boson with the interaction radius  $m_A^{-1}$  (where  $m_A$  is the mediator mass) much smaller than the object in which neutrinos propagate (or the distance over which the density varies), the Wolfenstein potential equals

$$V_W = \frac{g_\nu g_\psi}{m_A^2} n_\psi, \quad (1)$$

where  $n_\psi$  is the number density of the  $\psi$  particles,  $g_\nu$  and  $g_\psi$  are couplings of the mediator to  $\nu$  and  $\psi$  respectively. The potential depends on the local number density  $n_\psi$  while the size and shape of the object are not relevant. The medium can be considered as infinite. In the standard model (SM), the mediators are the  $W$  and  $Z$  bosons, satisfying the condition for (1). New heavy particles beyond the SM can generate via non-standard interactions additional contributions to the Wolfenstein potential with the same form as (1).

New neutrino interactions may be mediated by light particles as well, if the light mediators are very weakly coupled to the SM fermions. With sufficiently small values of  $g_\nu$  and  $g_\psi$  and correspondingly small  $m_A$ , sizable  $g_\nu g_\psi / m_A^2$  can evade various bounds from processes with large momentum transfer  $|q^2| \gg m_A^2$ , because the new physics contributions in such processes are typically proportional to the suppressed quantity  $g_\nu g_\psi / |q^2|$  rather than  $g_\nu g_\psi / m_A^2$ . By contrast, the Wolfenstein potential in (1), can be unchanged if  $m_A^2$  decreases proportionally with respect to  $g_\nu g_\psi$ . This, however, is restricted by the finite size of the object  $R$ . When  $m_A$  becomes smaller than  $1/R$ , the dependence of  $V_W$  on  $m_A$  in (1) is modified so that the matter effect turns out to be also suppressed. In this paper we will consider this dependence and its implications in details.

The matter effects due to light mediators have been studied before [4–20]. The mediators mostly considered in the literature are new gauge bosons of the lepton numbers  $L_e - L_\mu$ ,  $L_\mu - L_\tau$  or  $L_\tau - L_e$ . Long-range forces induced by these bosons can affect solar and atmospheric neutrino oscillations [4, 5] as well as high energy astrophysical neutrinos interacting with electrons in the Universe [14]. Various fifth force and gravitational experiments put very strong bounds on couplings of

light mediators with matter but in certain ranges it is neutrino oscillation phenomena that have the best sensitivity to couplings [16]. As for scalar interactions, it has been well known that the corresponding matter effect leads to corrections to the neutrino masses. Ref. [17] recently studied this scenario and showed that such interactions could explain the discrepancy between the solar neutrino and KamLAND measurements.

In this paper, we present detailed study of the Wolfenstein potentials induced by light mediators (both vector and scalar). We compute the Wolfenstein potentials for several spherically symmetric density profiles and study dependence of the potentials on the mediator mass. Taking into account existing bounds on light mediators, we assess their relevance to neutrino experiments.

The paper is organized as follows. In Sec. II we study the effects of light scalar and vector mediators on neutrino propagation, considering general matter density distributions. In Sec. III we present derivation of the effective potentials for several spherically symmetric density distributions which can be applied to the Earth, the Sun and similar celestial bodies. In Sec. IV we consider existing bounds on light mediators and apply our results to neutrinos propagating in the Sun and the Earth. Discussion and conclusions are presented in Sec. V.

## II. EFFECTS OF LIGHT MEDIATORS ON NEUTRINO PROPAGATIONS

Let us consider interactions between neutrinos ( $\nu$ ) and particles in matter ( $\psi$ ) mediated by a new light vector boson  $A^\mu$  or scalar boson  $\phi$ . The relevant part of the Lagrangian reads

$$\mathcal{L} \supset \bar{\nu} i \not{\partial} \nu - m_\nu \bar{\nu} \nu - g_\nu \bar{\nu} \not{A} \nu - g_\psi \bar{\psi} \not{A} \psi - \frac{m_A^2}{2} A^\mu A_\mu, \quad (2)$$

in the vector case. In the case of a scalar mediator, the last three terms in (2) should be replaced by

$$\mathcal{L} \supset -y_\nu \bar{\nu} \phi \nu - y_\psi \bar{\psi} \phi \psi - \frac{m_\phi^2}{2} \phi^2. \quad (3)$$

We assume that neutrinos are Dirac particles. For Majorana neutrinos, though the interaction forms are slightly different, the results are essentially the same. Also we consider neutrinos of a single flavor. It can be straightforwardly generalized to the case of three-neutrino mixing.

The Lagrangian (2) determines the equations of motion (EOM) of  $\nu$  and  $A^\mu$ :

$$i \not{\partial} \nu - m_\nu \nu - g_\nu \not{A} \nu = 0, \quad (4)$$

$$[\partial^2 + m_A^2] A^\mu - g_\nu \bar{\nu} \gamma_\mu \nu - g_\psi \bar{\psi} \gamma_\mu \psi = 0. \quad (5)$$

According to Eq. (4), the effect of  $A^\mu$  on neutrino propagation can be described as the displacement  $i \not{\partial} \rightarrow i \not{\partial} - g_\nu \not{A}$ , which in the momentum space corresponds to

$$p^\mu \rightarrow p^\mu + g_\nu A^\mu, \quad (6)$$

where  $p^\mu$  is the 4-momentum of the neutrino. In particular, the neutrino energy  $E$  receives the correction:

$$E = p^0 \rightarrow E + V, \quad V = g_\nu A^0. \quad (7)$$

In the scalar case, the EOM from Eq. (3) are

$$i \not{\partial} \nu - m_\nu \nu - y_\nu \phi \nu = 0, \quad (8)$$

$$[\partial^2 + m_\phi^2] \phi - y_\nu \bar{\nu} \nu - y_\psi \bar{\psi} \psi = 0. \quad (9)$$

As follows from Eq. (8), the effect of  $\phi$  on neutrino propagation is equivalent to changing the neutrino mass:

$$m_\nu \rightarrow m_\nu + \delta m_\nu, \quad \delta m_\nu = y_\nu \phi. \quad (10)$$

In most applications, the medium particles  $\psi$  are at rest (non-relativistic), hence

$$\bar{\psi}\psi = n_\psi, \quad \bar{\psi}\gamma^\mu\psi = n_\psi(1, 0, 0, 0). \quad (11)$$

Since the neutrino number density is much smaller than the number density of electrons or nucleons, we can assume  $\bar{\nu}\nu \ll \bar{\psi}\psi$  and  $\bar{\nu}\gamma_\mu\nu \ll \bar{\psi}\gamma_\mu\psi$  in Eqs. (9) and (5). This means that  $\phi$  and  $A^\mu$  are dominantly induced by  $\psi$ .

For the vector case, Eq. (11) implies that the spatial components of  $A^\mu$  vanish (up to gauge uncertainties):

$$A^\mu = (A^0, 0, 0, 0). \quad (12)$$

Furthermore, since the  $\psi$  particles are at rest,  $A^0$  has no temporal dependence ( $\partial_t A^0 = 0$ ). Therefore, Eq. (5) becomes

$$[-\nabla^2 + m_A^2] A^0 = g_\psi n_\psi. \quad (13)$$

Given a distribution of  $n_\psi$ , Eq. (13) determines the distribution of  $A^0$ .

All the above analyses can be straightforwardly applied to a scalar mediator. Starting from Eq. (9), we obtain an equation similar to Eq. (13):

$$[-\nabla^2 + m_\phi^2] \phi = y_\psi n_\psi, \quad (14)$$

and hence a similar solution.

From Eqs. (13) and (14), we can see that  $\phi$  and  $A^0$  are determined by  $n_\psi$  in almost the same way. However, the effects of  $\phi$  and  $A^0$  on neutrino propagation are very different.

In the evolution equation of neutrino oscillation,  $\phi$  gives correction to the mass and changes  $(m_\nu)^2/2E$  in the oscillation phase to  $(m_\nu + \delta m_\nu)^2/2E$ , approximately (for  $\delta m_\nu \ll m_\nu$ ) corresponding to adding

$$V_S \approx \frac{m_\nu}{E} \delta m_\nu = \frac{m_\nu}{E} y_\nu \phi, \quad (15)$$

to  $(m_\nu)^2/2E$ . In comparison, the effect of  $A^0$  is included by directly adding  $V = g_\nu A^0$  to  $(m_\nu)^2/2E$ . Thus, the scalar matter effect enters the flavor evolution equation with the additional suppression factor  $m_\nu/E$ . The factor  $m_\nu/E$  is due to chiral suppression. Since the helicity is conserved in neutrino oscillations, the chirality-flipping terms in the Lagrangian, such as neutrino masses or scalar interactions, have to change it twice, which is the reason that  $m_\nu^2$  appears instead of  $m_\nu$  in neutrino oscillations. Because the scalar interaction flips the chirality, another flip is needed which is given by  $m_\nu/2E$ . In other words, only  $m_\nu/2E$  fraction of the chirality-flipped state contains the original helicity. This means that, to obtain effects of the same size,  $y_\nu \phi$  should be  $\frac{E}{m_\nu}$  times larger than  $g_\nu A^0$ . That is,  $y_\nu y_\psi/m_\phi^2$  should be  $\frac{E}{m_\nu}$  times larger than  $g_\nu g_\psi/m_A^2$ . This strongly affects the relevance of the scalar case to the oscillation phenomenology.

### III. EFFECTIVE POTENTIALS FOR SPHERICALLY SYMMETRIC DENSITY DISTRIBUTIONS

In what follows, we focus our discussion on the vector case, while for the scalar case, the results can be obtained immediately with the substitutions:  $A^0 \rightarrow \phi$ ,  $m_A \rightarrow m_\phi$ ,  $g_\nu \rightarrow y_\nu$ , and  $g_\psi \rightarrow y_\psi$ .

In many applications (e.g., the Earth, the Sun), the matter density distribution is, to a good approximation, spherically symmetric. The spherical symmetry allows us to reduce Eq. (13) to a radial differential equation:

$$\left[ \frac{\partial^2}{\partial r^2} + \frac{2\partial}{r\partial r} - m_A^2 \right] A^0(r) = -g_\psi n_\psi(r). \quad (16)$$

For any given profile  $n_\psi(r)$ , Eq. (16) can be solved by a standard method known as *variation of parameters*, which gives

$$\begin{aligned} A^0(r) = & g_\psi \frac{e^{-m_A r}}{m_A r} \int_0^r x n_\psi(x) \sinh(m_A x) dx \\ & + g_\psi \frac{\sinh(m_A r)}{m_A r} \int_r^\infty x n_\psi(x) e^{-m_A x} dx. \end{aligned} \quad (17)$$

The above computations of potentials are essentially classical. Therefore for an arbitrary density distribution  $n_\psi(\mathbf{r})$  (not necessarily spherically symmetric),  $A^0$  can be found by performing summation (integration) of the contributions of individual particles  $\psi$  [see also Eq. (23)]:

$$A^0(\mathbf{r}) = -\frac{g_\psi}{4\pi} \int n_\psi(\tilde{\mathbf{r}}) \frac{e^{-m_A |\mathbf{r} - \tilde{\mathbf{r}}|}}{|\mathbf{r} - \tilde{\mathbf{r}}|} d^3\tilde{\mathbf{r}}. \quad (18)$$

For the spherically symmetric case, one can integrate over angular variables in Eq. (18), which also leads to Eq. (17).

Now let us compute the Wolfenstein potentials explicitly for several density profiles, which can be used to approximately describe the matter density distributions of the Earth, the Sun, and similar celestial bodies. Some interesting limits will also be discussed.

#### ■ Constant density within a sphere

For a constant density distribution within a sphere of radius  $R$ :

$$n_\psi(r) = \begin{cases} 0 & (\text{for } r > R) \\ n_\psi & (\text{for } r \leq R) \end{cases}, \quad (19)$$

we find from (17)

$$A^0(r) = \frac{g_\psi n_\psi}{m_A^2} F(r), \quad (20)$$

where

$$F(r) = \begin{cases} 1 - \frac{m_A R + 1}{m_A r} e^{-m_A R} \sinh(m_A r) & (r \leq R) \\ \frac{e^{-m_A r}}{m_A r} [m_A R \cosh(m_A R) - \sinh(m_A R)] & (r > R) \end{cases}, \quad (21)$$

describes deviation from the infinite medium potential. Then according to Eq. (7), the effective neutrino potential produced by  $A^0$  equals

$$V(r) = g_\nu A^0(r) = \frac{g_\nu g_\psi n_\psi}{m_A^2} F(r). \quad (22)$$

Several important limits are in order.

- $R \rightarrow 0$  with a constant particle number of  $\psi$ .

We consider the particle number  $N_\psi \equiv \frac{4}{3}\pi R^3 n_\psi$  within the sphere is a constant when taking  $R \rightarrow 0$ . In this limit,  $n_\psi(r) \rightarrow N_\psi \delta(r)$ , and Eqs. (21) and (22) give

$$V(r) = \frac{g_\nu g_\psi}{m_A^2} \frac{e^{-m_A r}}{r} n_\psi \frac{R^3}{3} = \frac{g_\nu g_\psi}{m_A^2} N_\psi \frac{e^{-m_A r}}{4\pi r}, \quad (23)$$

which, for  $N_\psi = 1$ , reproduces the Yukawa potential of a single  $\psi$  particle.

- $m_A \rightarrow 0$ .

In the limit of massless mediator, Eqs. (21) and (22) lead to

$$V(r) = g_\nu g_\psi n_\psi \times \begin{cases} \frac{3R^2 - r^2}{6} & (r \leq R) \\ \frac{R^3}{3r} & (r > R) \end{cases}. \quad (24)$$

which coincides with the  $r$  dependence of the Coulomb potential of a charged sphere. Actually in this limit, the potential for  $r > R$  is determined by the total particle number  $N_\psi$  inside the sphere, independent of the radial distribution. If  $m_A$  is nonzero but small, the first order correction in  $m_A$  to the potential equals (for both  $r \leq R$  and  $r > R$ )

$$\delta V(r) = -g_\nu g_\psi n_\psi \frac{m_A}{3} R^3. \quad (25)$$

- $m_A \rightarrow \infty$ .

In this limit, Eqs. (21) and (22) give

$$V(r) = \begin{cases} \frac{g_\nu g_\psi n_\psi}{m_A^2} & (r \leq R) \\ 0 & (r > R) \end{cases}. \quad (26)$$

Inside the medium, the potential is a constant and outside it vanishes. This reproduces the standard Wolfenstein potential for infinite medium.

- $|R - r| \ll m_A^{-1} \ll R$ .

Here  $R - r$  can be interpreted as the depth of neutrino trajectory. Hence the limit means the radius of interactions is much smaller than  $R$  but much larger than the depth of the trajectory. The absolute sign “ $|$ ” indicates that this limit applies not only to underground neutrino trajectories but also to above-the-surface neutrino beams. The limit can be realized for reactor and accelerator experiments.

In this limit, we obtain

$$V(r) = \frac{1}{2} \frac{g_\nu g_\psi n_\psi}{m_A^2}. \quad (27)$$

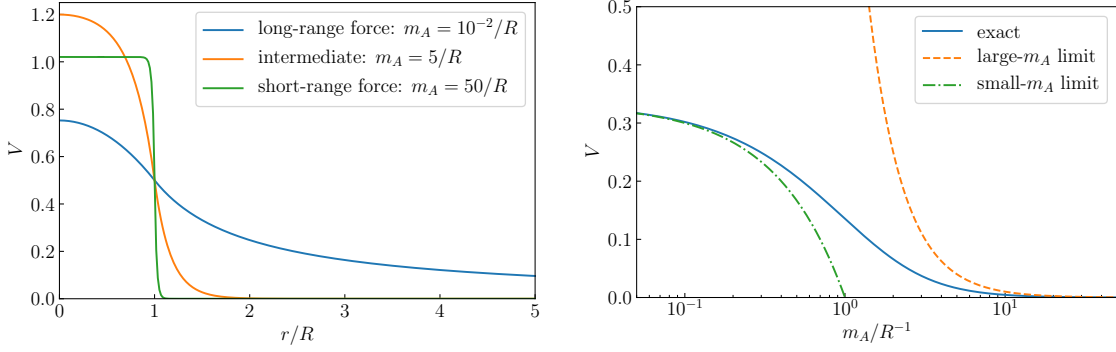


Figure 1. The effective potentials  $V$  (in arbitrary unit) produced by a sphere of radius  $R$  with constant matter density. *Left panel:* Dependence of  $V$  on the distance  $r$ , for different values of the mediator mass  $m_A$ . *Right panel:* Comparison of  $V(m_A)$  in the large- $m_A$  and small- $m_A$  limits with the exact result, computed using Eqs. (20)-(22) and (24)-(26) at the surface of the sphere ( $r = R$ ). Values of  $g_\nu g_\psi n_\psi$  are chosen in such a way that  $V(r = R) = 1/2$  for all values of  $m_A$ .

It differs from the standard Wolfenstein potential by the additional factor of  $1/2$ , which reflects that only half of the space produces the potential.

In the left panel of Fig. 1, we show the dependence of  $V$  on  $r$  for different values of  $m_A$  according to (22) and (21). For  $m_A \gg R^{-1}$  (green curve), the  $r$ -dependence is close to that of the standard Wolfenstein potential, which is essentially a step function. When  $m_A$  decreases, it becomes smoother (yellow line). For very small  $m_A$ , the long-range force leads to a Column-like potential (blue curve). Near the surface ( $r \approx R$ ) the short-range potential (green curve) is roughly half the standard Wolfenstein potential (the plateau of this curve), as expected from Eq. (27).

In the right panel of Fig. 1, we show the dependence of  $V$  at  $r = R$  on  $m_A$  according to the exact formula (blue solid curve) as well as the small- and large- $m_A$  limits in Eqs. (24)-(26). The inverse-square dependence on  $m_A$  of the standard Wolfenstein potential deviates significantly from the exact potential for small  $m_A$ .

## ■ Multi-layer density profile

A multi-layer density profile is a good approximation for the Earth. Using result (21) for constant density sphere one can write up results for the Earth density profile with several spherical layers of different density. For instance, for two layers (a simplified mantle-core profile) with constant average densities  $n_\psi^M$  and  $n_\psi^C$  and radii  $R^M$  and  $R^C$  respectively, the Wolfenstein potential in the mantle is

$$V(r) = \frac{g_\nu g_\psi}{m_A^2} [n_\psi^M F_{r < R}(r, R^M) + (n_\psi^C - n_\psi^M) F_{r > R}(r, R^C)], \quad (28)$$

and in the core is

$$V(r) = \frac{g_\nu g_\psi}{m_A^2} [n_\psi^M F_{r < R}(r, R^M) + (n_\psi^C - n_\psi^M) F_{r < R}(r, R^C)], \quad (29)$$

where  $F_{r < R}$  and  $F_{r > R}$  are given by the lower and the upper lines of Eq. (21). For more realistic profiles with many layers, the generalization is straightforward.

## ■ Exponential density distribution

Exact analytic results can be obtained for an exponential density distribution,

$$n_\psi(r) = n_\psi(0)e^{-r\kappa}. \quad (30)$$

This distribution can be used to partially describe the matter density of the Sun and some celestial bodies. Computing the integral in (17) gives

$$V(r) = \frac{g_\nu g_\psi n_\psi(r)}{m_A^2 - \kappa^2} \left[ 1 + \frac{2\kappa}{m_A^2 - \kappa^2} \frac{1}{r} \left( e^{(\kappa - m_A)r} - 1 \right) \right]. \quad (31)$$

Several important limits are in order.

- $\kappa \rightarrow 0$ .

This limit is actually a constant density distribution. In this limit, Eq. (31) reduces to the standard Wolfenstein potential of infinite medium, see Eq. (26) with  $n_\psi = n_\psi(0)$ .

- $m_A \ll \kappa$ .

In this limit, the range of the force is much larger than the scale of density variation. From Eq. (31), we obtain

$$V(r) = -\frac{g_\nu g_\psi n_\psi(r)}{\kappa^2} \left[ 1 - \frac{2}{\kappa r} (e^{\kappa r} - 1) \right], \quad (32)$$

which does not depend on  $m_A$ .

For  $r \gg \kappa^{-1}$ , Eq. (32) reduces to

$$V(r) = \frac{g_\nu g_\psi n_\psi(0)}{\kappa^2} \frac{2}{\kappa r}, \quad (33)$$

which means that the potential at large  $r$  decreases as  $1/r$ , i.e., slower than the matter density ( $\propto e^{-\kappa r}$ ) decreases. This can produce interesting phenomena such as new level crossing for solar neutrinos [21].

- $m_A \approx \kappa$ .

In this limit, Eq. (31) gives

$$V(r) = \frac{g_\nu g_\psi n_\psi(r)}{4\kappa^2} (1 + \kappa r). \quad (34)$$

## ■ Exponential density distribution with a cut-off

The matter density in the Sun can be more accurately formulated as an exponential distribution with a cut-off roughly correspond to the solar radius. Hence we consider:

$$n_\psi(r) = n_\psi(0) \begin{cases} e^{-r\kappa} & (r \leq R) \\ 0 & (r > R) \end{cases}. \quad (35)$$

After straightforward calculations, we obtain the potential:

$$V(r) = \frac{g_\nu g_\psi n_\psi(0)}{m_A r} \times \begin{cases} K_{\text{in}} & (r \leq R) \\ K_{\text{out}} & (r > R) \end{cases}, \quad (36)$$

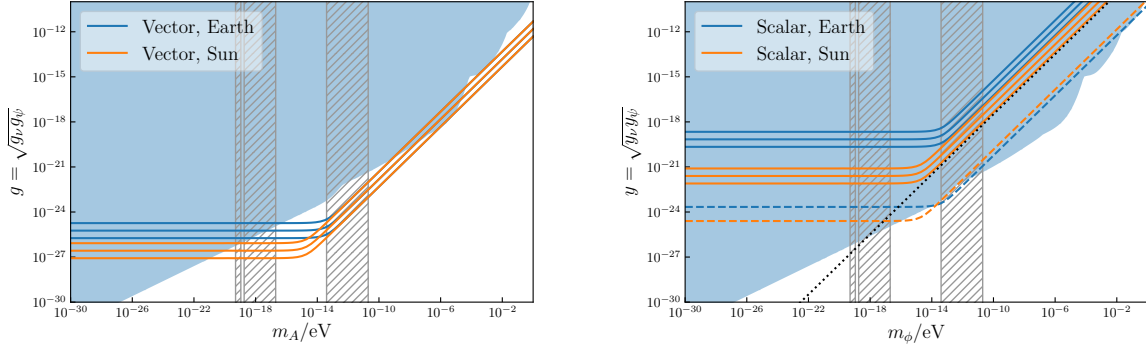


Figure 2. The parameter space for ultra-light vector (left) and scalar (right) mediators to generate significant matter effects. Left: from up to down, the solid curves correspond to  $V/V_{\text{SM}} \in \{10^{-2}, 10^{-1}, 1\}$ . Right: from up to down, the solid curves correspond to  $\delta m_\nu/\text{eV} \in \{10^{-3}, 10^{-2}, 10^{-1}\}$ . The blue shaded regions are excluded by the combination of various observations (explained in the text). The grey hatched region is excluded by black hole super-radiance. For comparison, we plot two dashed lines with much smaller values of  $\delta m_\nu/\text{eV}$  that can exceed the blue region ( $\delta m_\nu = 10^{-11}$  eV for the Earth and  $\delta m_\nu = 10^{-8}$  eV for the Sun), though this is far beyond the precision of any realistic experiments.

with  $K_{\text{in}}$  and  $K_{\text{out}}$  given by

$$K_{\text{in}} \equiv \kappa m_A e^{-r(\kappa+m_A)} \frac{e^{m_A r} (m_A^2 r \kappa^{-1} - \kappa r - 2) + 2e^{\kappa r}}{(m_A^2 - \kappa^2)^2} - \frac{\sinh(m_A r) e^{-R(\kappa+m_A)} (m_A R + \kappa R + 1)}{(m_A + \kappa)^2}, \quad (37)$$

$$K_{\text{out}} \equiv e^{-m_A r - \kappa R} \sinh(m_A R) \frac{m_A^2 (\kappa R - 1) - \kappa^2 (\kappa R + 1)}{(m_A^2 - \kappa^2)^2} + e^{-m_A r - \kappa R} \cosh(m_A R) \frac{m_A^3 R - \kappa^2 R m_A - 2\kappa m_A}{(m_A^2 - \kappa^2)^2} + e^{-m_A r} \frac{2\kappa m_A}{(m_A^2 - \kappa^2)^2}. \quad (38)$$

All the above results can be applied to the scalar case with the simple substitution:  $A^0 \rightarrow \phi$ ,  $m_A \rightarrow m_\phi$ ,  $g_\nu \rightarrow y_\nu$ , and  $g_\psi \rightarrow y_\psi$ .

#### IV. PHENOMENOLOGY

Let us consider experimental bounds on the couplings and masses of light mediators and check whether light scalar and vector mediators, that satisfy these bounds, can produce observable matter effects in neutrino oscillations. For brevity we introduce the couplings  $g \equiv \sqrt{g_\nu g_\psi}$  and  $y \equiv \sqrt{y_\nu y_\psi}$ .

For  $m_{A,\phi} \gtrsim \mathcal{O}(10^2)$  keV,  $g^2/m_A^2 \gtrsim G_F$  and  $y^2/m_\phi^2 \gtrsim G_F$  have been excluded by numerous laboratory experiments including elastic neutrino-electron scattering [22–24], neutrino-nucleus scattering [25–27], fixed target experiments [28–30], collider searches [31, 32], etc. For  $1 \text{ eV} \lesssim m_{A,\phi} \lesssim 10^2 \text{ keV}$ , the astrophysical observations provide much stronger constraints. For instance, the expected amount of energy loss via neutrinos in the Sun and globular clusters excludes  $g$  and  $y$  down to  $10^{-14}$ , corresponding to an upper bound of  $g^2/m_A^2$  or  $y^2/m_\phi^2$  above  $10^{-5} G_F$  [33].

Below 1 eV, the constraints mainly come from searches of fifth forces and precision tests of gravity [34, 35]. These constraints are only applicable to  $g_\psi$  or  $y_\psi$ . To obtain the bounds on  $\sqrt{g_\nu g_\psi}$



or  $\sqrt{y_\nu y_\psi}$ , we can use the cosmological bounds on neutrino self-interactions,  $g_\nu^2/m_A^2$  or  $y_\nu^2/m_\phi^2 \lesssim (3 \text{ MeV})^{-2}$  [36]. In addition, for certain ranges of  $m_{A,\phi}$ , black hole super-radiance provides robust constraints [14, 37] which are independent of the couplings. These constraints are combined and presented in Fig. 2.

Now let us determine the required values of  $g_\nu g_\psi$  or  $y_\nu y_\psi$  to generate significant matter effects, which can be quantified by

$$\frac{V}{V_{\text{SM}}} = \frac{g^2}{m_A^2 \sqrt{2} G_F} F(r, m_A^2), \quad \delta m_\nu = \frac{y^2}{m_\phi^2} n_\psi(r) F(r, m_\phi^2). \quad (39)$$

where  $V_{\text{SM}} \equiv \sqrt{2} G_F n_\psi$ , and  $F$  describes the deviation from the standard Wolfenstein potential. According to Eq. (39), given specific values of  $\frac{V}{V_{\text{SM}}}$  and  $\delta m_\nu$ ,  $g^2$  and  $y^2$  are determined by:

$$g^2 = \frac{V}{V_{\text{SM}}} m_A^2 \sqrt{2} G_F F^{-1}(r, m_A^2), \quad y^2 = \delta m_\nu m_\phi^2 [n_\psi(r) F(r, m_\phi^2)]^{-1}. \quad (40)$$

We take  $V/V_{\text{SM}} \in \{10^{-2}, 10^{-1}, 1\}$  and  $\delta m_\nu \in \{10^{-3}, 10^{-2}, 10^{-1}\} \text{ eV}$  and plot the corresponding curves in Fig. 2. The value of  $F$  has been computed numerically using the density distributions for the Sun from [38] and for the Earth from [39]. The value of  $r$  is set to zero for the Sun, and to the Earth radius for the Earth.

The  $g$ - $m_A$  or  $y$ - $m_\phi$  curves can be understood from our analytic results. For large  $m_A$  (short range forces),  $F \approx 1$ . According to Eq. (40), we have  $g \propto m_A^2$  for  $m_A \ll 1/R$ , where  $R$  is the radius of the object. For very small  $m_A$ ,  $F$  should be proportional to  $m_A^2$  so that  $g$  is independent of  $m_A$ . In the intermediate range,  $m_A \sim 1/R$ , the dependence is more complicated.

From Fig. 2, we can see that the solid curves which take into account finite sizes of the Sun or the Earth, turn to be horizontal below  $10^{-16} \text{ eV}$  or  $10^{-14} \text{ eV}$  respectively. Note that the solar radius  $R_\odot = 7.0 \times 10^5 \text{ km}$  and the earth radius  $R_\oplus \approx 6.4 \times 10^3 \text{ km}$  correspond to the mass scales  $2.8 \times 10^{-16} \text{ eV}$  and  $3.1 \times 10^{-14} \text{ eV}$  respectively. Below these scales, the potentials are essentially generated by long-range forces and no longer sensitive to the mediator masses.

Fig. 2 shows that for vector mediators, there is an allowed region of  $m_A$  for strong matter effects:  $[2 \times 10^{-17}, 4 \times 10^{-14}] \text{ eV}$ . This could motivate further phenomenological studies. Scalar interactions, however, cannot generate significant matter effects, in contrast to the claim in Ref. [17]. For illustration, we plot a black dotted line which corresponds to infinite size medium, i.e., the Sun is assumed to be infinitely large. In this case, significant matter effects would be possible for  $m_\phi \lesssim 10^{-20} \text{ eV}$ . However, this possibility is excluded when the  $F(r)$  correction due to the finite size of medium is taken into account.

One may be interested in the actually allowed values of scalar matter effect. So we plot two dashed curves that can exceed the blue region, corresponding to  $\delta m_\nu = 10^{-11} \text{ eV}$  for the Earth and  $\delta m_\nu = 10^{-8} \text{ eV}$  for the Sun). These values are far beyond the precision of any realistic experiments.

Finally, we would like to comment that severe constraints on the scalar matter effect may also come from supernovae, which have not been considered in the literature. Let us estimate the effect in the core of a supernova, which has a typical radius of  $R_{\text{SN}} = 20 \sim 30 \text{ km}$  and a density of  $n_\psi^{\text{SN}} = 10^{13} \sim 10^{14} \text{ g/cm}^3$ . For relatively heavy scalar mediators with  $m_\phi > 1/R_{\text{SN}}$ , the mass correction is

$$\delta m_\nu^{\text{SN}} \sim \frac{n_\psi^{\text{SN}}}{n_\psi^{\text{earth}}} \delta m_\nu^{\text{earth}}, \quad (41)$$

which is about 13 orders of magnitude larger than the effect at the Earth  $\delta m_\nu^{\text{earth}}$ . For  $\delta m_\nu^{\text{earth}} = 0.01 \text{ eV}$ , we obtain  $\delta m_\nu^{\text{SN}} \sim 100 \text{ GeV}$ , which is certainly excluded since in this case neutrinos can not

even be produced in supernovae. For very light mediators with  $m_\phi < 1/R_{\text{SN}}$ , Eq. (41) is modified to

$$\delta m_\nu^{\text{SN}} \sim \frac{n_\psi^{\text{SN}}}{n_\psi^{\text{earth}}} \left( \frac{R^{\text{SN}}}{R^{\text{earth}}} \right)^2 \delta m_\nu^{\text{earth}}. \quad (42)$$

Taking  $\delta m_\nu^{\text{earth}} = 0.01$  eV, we obtain  $\delta m_\nu^{\text{SN}} = 1$  MeV and correspondingly  $y = 10^{-28}$ . Therefore in this case,  $y \gtrsim 10^{-28}$  can be roughly excluded. More detailed analyses will be given in our future work [21].

## V. CONCLUSION

We study the effects of new neutrino-matter interactions mediated by ultra-light scalar and vector bosons on neutrino propagation, taking the finite size and density distribution of the medium into consideration. We compute the Wolfenstein potentials explicitly for several spherically symmetric density profiles which can be approximately applied to the Earth and the Sun.

The Wolfenstein potentials induced by ultra-light mediators have very different dependence on the mediator masses ( $m_A$ ) from the standard case. In infinite medium, due to the  $1/m_A^2$  dependence in Eq. (1), the Wolfenstein potentials can be enhanced by reducing the mediator masses. In finite medium of size  $R$ , when  $m_A$  decreases to the ultra-light region where  $m_A^{-1}$  becomes comparable or larger than  $R$ , the  $1/m_A^2$  dependence is modified. In this case the matter effect is determined not only by the local density, but also by the geometry (including the size and density distribution) of the object. In particular, the potential can extend outside of the medium. For  $m_A \ll R$ , the potential does not depend on  $m_A$ .

With correct expressions for the Wolfenstein potentials and existing bounds on light mediators, we find that scalar interactions cannot generate observable effects in realistic experiments, which implies that the scenario considered in Ref. [17] is not viable. Vector mediators, however, can produce significant matter effect at least within the parameter space  $m_A \in [2 \times 10^{-17}, 4 \times 10^{-14}]$  eV and  $g \sim 10^{-25}$ .

- 
- [1] L. Wolfenstein, *Phys.Rev.* **D17**, 2369 (1978).
  - [2] S. Mikheev and A. Y. Smirnov, *Sov.J.Nucl.Phys.* **42**, 913 (1985).
  - [3] S. Mikheev and A. Y. Smirnov, *Nuovo Cim.* **C9**, 17 (1986).
  - [4] A. S. Joshipura and S. Mohanty, *Phys. Lett.* **B584**, 103 (2004), [arXiv:hep-ph/0310210 \[hep-ph\]](#).
  - [5] J. A. Grifols and E. Masso, *Phys. Lett.* **B579**, 123 (2004), [arXiv:hep-ph/0311141 \[hep-ph\]](#).
  - [6] A. Bandyopadhyay, A. Dighe, and A. S. Joshipura, *Phys. Rev.* **D75**, 093005 (2007), [arXiv:hep-ph/0610263 \[hep-ph\]](#).
  - [7] M. C. Gonzalez-Garcia, P. C. de Holanda, E. Masso, and R. Zukanovich Funchal, *JCAP* **0701**, 005 (2007), [arXiv:hep-ph/0609094 \[hep-ph\]](#).
  - [8] A. E. Nelson and J. Walsh, *Phys. Rev.* **D77**, 033001 (2008), [arXiv:0711.1363 \[hep-ph\]](#).
  - [9] M. C. Gonzalez-Garcia, P. C. de Holanda, and R. Zukanovich Funchal, *JCAP* **0806**, 019 (2008), [arXiv:0803.1180 \[hep-ph\]](#).
  - [10] A. Samanta, *JCAP* **1109**, 010 (2011), [arXiv:1001.5344 \[hep-ph\]](#).
  - [11] H. Davoudiasl, H.-S. Lee, and W. J. Marciano, *Phys. Rev.* **D84**, 013009 (2011), [arXiv:1102.5352 \[hep-ph\]](#).
  - [12] H.-S. Lee, *Proceedings, 13th International Workshop on Neutrino Factories, Superbeams and Beta beams (NuFact11): Geneva, Switzerland, August 1-6, 2011*, *J. Phys. Conf. Ser.* **408**, 012032 (2013), [arXiv:1110.1335 \[hep-ph\]](#).
  - [13] S. S. Chatterjee, A. Dasgupta, and S. K. Agarwalla, *JHEP* **12**, 167 (2015), [arXiv:1509.03517 \[hep-ph\]](#).

- [14] M. Bustamante and S. K. Agarwalla, *Phys. Rev. Lett.* **122**, 061103 (2019), [arXiv:1808.02042 \[astro-ph.HE\]](#).
- [15] A. Khatun, T. Thakore, and S. Kumar Agarwalla, *JHEP* **04**, 023 (2018), [arXiv:1801.00949 \[hep-ph\]](#).
- [16] M. B. Wise and Y. Zhang, *JHEP* **06**, 053 (2018), [arXiv:1803.00591 \[hep-ph\]](#).
- [17] S.-F. Ge and S. J. Parke, *Phys. Rev. Lett.* **122**, 211801 (2019), [arXiv:1812.08376 \[hep-ph\]](#).
- [18] G. Krnjaic, P. A. N. Machado, and L. Necib, *Phys. Rev.* **D97**, 075017 (2018), [arXiv:1705.06740 \[hep-ph\]](#).
- [19] A. Berlin, *Phys. Rev. Lett.* **117**, 231801 (2016), [arXiv:1608.01307 \[hep-ph\]](#).
- [20] V. Brdar, J. Kopp, J. Liu, P. Prass, and X.-P. Wang, *Phys. Rev.* **D97**, 043001 (2018), [arXiv:1705.09455 \[hep-ph\]](#).
- [21] A. Y. Smirnov and X.-J. Xu, work in preparation (2019).
- [22] W. Rodejohann, X.-J. Xu, and C. E. Yaguna, *JHEP* **05**, 024 (2017), [arXiv:1702.05721 \[hep-ph\]](#).
- [23] M. Lindner, F. S. Queiroz, W. Rodejohann, and X.-J. Xu, *JHEP* **05**, 098 (2018), [arXiv:1803.00060 \[hep-ph\]](#).
- [24] G. Arcadi, M. Lindner, J. Martins, and F. S. Queiroz, (2019), [arXiv:1906.04755 \[hep-ph\]](#).
- [25] M. Lindner, W. Rodejohann, and X.-J. Xu, *JHEP* **03**, 097 (2017), [arXiv:1612.04150 \[hep-ph\]](#).
- [26] Y. Farzan, M. Lindner, W. Rodejohann, and X.-J. Xu, *JHEP* **05**, 066 (2018), [arXiv:1802.05171 \[hep-ph\]](#).
- [27] V. Brdar, W. Rodejohann, and X.-J. Xu, *JHEP* **12**, 024 (2018), [arXiv:1810.03626 \[hep-ph\]](#).
- [28] J. D. Bjorken, R. Essig, P. Schuster, and N. Toro, *Phys. Rev.* **D80**, 075018 (2009), [arXiv:0906.0580 \[hep-ph\]](#).
- [29] B. Batell, M. Pospelov, and A. Ritz, *Phys. Rev.* **D80**, 095024 (2009), [arXiv:0906.5614 \[hep-ph\]](#).
- [30] R. Essig, R. Harnik, J. Kaplan, and N. Toro, *Phys. Rev.* **D82**, 113008 (2010), [arXiv:1008.0636 \[hep-ph\]](#).
- [31] J. P. Lees *et al.* (BaBar), *Phys. Rev. Lett.* **113**, 201801 (2014), [arXiv:1406.2980 \[hep-ex\]](#).
- [32] J. P. Lees *et al.* (BaBar), *Phys. Rev.* **D94**, 011102 (2016), [arXiv:1606.03501 \[hep-ex\]](#).
- [33] R. Harnik, J. Kopp, and P. A. N. Machado, *JCAP* **1207**, 026 (2012), [arXiv:1202.6073 \[hep-ph\]](#).
- [34] E. G. Adelberger, B. R. Heckel, S. A. Hoedl, C. D. Hoyle, D. J. Kapner, and A. Upadhye, *Phys. Rev. Lett.* **98**, 131104 (2007), [arXiv:hep-ph/0611223 \[hep-ph\]](#).
- [35] S. Schlamminger, K. Y. Choi, T. A. Wagner, J. H. Gundlach, and E. G. Adelberger, *Phys. Rev. Lett.* **100**, 041101 (2008), [arXiv:0712.0607 \[gr-qc\]](#).
- [36] C. D. Kreisch, F.-Y. Cyr-Racine, and O. Dore, (2019), [arXiv:1902.00534 \[astro-ph.CO\]](#).
- [37] M. Baryakhtar, R. Lasenby, and M. Teo, *Phys. Rev.* **D96**, 035019 (2017), [arXiv:1704.05081 \[hep-ph\]](#).
- [38] J. Edsjo, J. Elevant, R. Enberg, and C. Niblaeus, *JCAP* **1706**, 033 (2017), [arXiv:1704.02892 \[astro-ph.HE\]](#).
- [39] A. M. Dziewonski and D. L. Anderson, *Phys. Earth Planet. Interiors* **25**, 297 (1981).